Appl Biochem Biotechnol (2016) 179:1–15
DOI 10.1007/s12010-015-1975-6

Characterization and Soluble Expression of D-Hydantoinase from *Pseudomonas fluorescens* for the Synthesis of D-Amino Acids

Guo-Chao Xu[1] · Lei Li[1] · Rui-Zhi Han[1] · Jin-Jun Dong[1] · Ye Ni[1]

Received: 21 October 2015 / Accepted: 29 December 2015 /
Published online: 28 January 2016

Abstract An active D-hydantoinase from *Pseudomonas fluorescens* was heterogeneously overexpressed in *Escherichia coli* BL21(DE3) and designated as D-*Pf*HYD. Sequence and consensus analysis suggests that D-*Pf*HYD belongs to the dihydropyrimidinase/hydantoinase family and possesses catalytic residues for metal ion and hydantoin binding. D-*Pf*HYD was purified to homogeneity by nickel affinity chromatography for characterization. D-*Pf*HYD is a homotetramer with molecular weight of 215 kDa and specific activity of 20.9 U mg^{-1}. D-*Pf*HYD showed the highest activity at pH 9.0 and 60 °C. Metal ions such as Mn^{2+}, Fe^{2+}, and Fe^{3+} could activate D-*Pf*HYD with 20 % improvement. Substrate specificity analysis revealed that purified D-*Pf*HYD preferred aliphatic to aromatic 5′-monosubstituted hydantoins. Among various strategies tested, chaperone GroES-GroEL was efficient in improving the soluble expression of D-*Pf*HYD. Employing 1.0 g L^{-1} recombinant *E. coli* BL21(DE3)-pET28-*hyd*/pGRO7 dry cells, 100 mM isobutyl hydantoin was converted into D-isoleucine with 98.7 % *enantiomeric excess* (*ee*), isolation yield of 78.3 %, and substrate to biocatalyst ratio of 15.6. Our results suggest that recombinant D-*Pf*HYD could be potentially applied in the synthesis of D-amino acids.

Keywords *Pseudomonas fluorescens* · D-hydantoinase · D-amino acids · Soluble expression · Chaperone

Electronic supplementary material The online version of this article (doi:10.1007/s12010-015-1975-6) contains supplementary material, which is available to authorized users.

✉ Ye Ni
yni@jiangnan.edu.cn

[1] The Key Laboratory of Industrial Biotechnology, Ministry of Education, School of Biotechnology, Jiangnan University, Wuxi 214122 Jiangsu, China

Introduction

Optically pure D-amino acids (D-AAs) are important amino acids, which distribute widely in gram-positive bacterial cell walls (peptidoglycan and poly-γ-glutamate, etc.) to protect them against proteolytic enzymes, as well as in plants and animals as opioid peptide and neuropeptide components [1]. D-AAs have been extensively used as key chiral intermediates for the synthesis of pharmaceuticals, agrochemicals, food additives, cosmetics, and fine chemicals. It's well known that aspoxicillin could be synthesized with D-Asp and amoxicillin, which has longer half-life and low serum protein-binding characteristics [2]. Alitame (L-Asp-D-Ala dipeptide), a popular sweetener for diabetics, is ten times more potent and has low calorie than Aspartame (L-Asp-L-Phe dipeptide) [3]. D-Glu and D-Ser can be used in cosmetics to help reduce wrinkle and ultraviolet damage [4]. D-Isoleucine is a key synthon for the synthesis of various chemical ligands, antibiotics, and bacitracins [5]. Therefore, the efficient production of chiral D-AAs is of great interest.

Various strategies have been developed, including chemical synthesis, fermentation, and enzymatic transformation [6]. The chemical methods are usually of high cost and low yields due to the dependence on chiral resolution catalysts [1]. It is difficult to obtain D-AAs of high optical purity and productivity by fermentation due to the complex enzymatic systems [7]. Biotransformation is regarded as a green and promising process for the production of D-AAs with high enantioselectivity, productivity, and isolation yield [8]. D-AAs could be enzymatically synthesized by D-hydantoinase, D-amidohydrolase, *N*-acyl-D-amino acid amidohydrolase, D-amino acid amidase, D-aminopeptidase, alkaline D-peptidase, L-amino acid oxidase, D-amino acid aminotransferase, and D-amino acid dehydrogenase [1]. Among them, "D-hydantoinase process" is industrially preferred due to its high enantioselectivity and potentially 100 % theoretical yield with racemic substrates [5, 8].

D-Hydantoinase (dihydropyrimidinase, EC 3.5.2.2), classified into cyclic amidase family, could catalyze the reversible ring opening hydrolysis of hydantoin and corresponding 5′-monosubstituted analogues and is widely distributed in bacteria, plants, and animals [9]. Since the 1940s, many hydantoinase (HYD)-producing microorganisms have been isolated by enrichment with hydantoin as sole carbon or nitrogen source, including *Pseudomonas putida* [10], *Agrobacterium tumefaciens* [11], *Bacillus stearothermophilus* [12], *Burkholderia pickettii* [13], *Arthrobacter aurescens* [14], etc., or even from plants such as *adzuki bean* [15] and pig liver [16]. The scale-up production of D-AAs is usually hindered by the low level of intracellular active enzymes and complex enzyme systems in wild-type strains. Studies on the heterogeneous overexpression, transposon mutagenesis, and genome data mining of D-hydantoinases (D-HYDs) are therefore of great importance [17]. Various D-HYDs have been identified and systemically characterized in the preparation of D-AAs with diverse substrate specificities. It has been reported that non-selective HYD from *B. stearothermophilus* and D-HYD from *Arthrobacter crystallopoietes* have substrate specificity toward alphatic 5′-substituted hydantoin derivatives [12, 18] and D-HYDs from *Pseudomonas putida* and *Agrobacterium* sp. prefer aromatic 5′-substituted hydantoins [19, 20], while HYD from *Arthrobacter aurescens* displays substrate-dependent enantioselectivity [14]. Besides, most of the D-HYD-coding genes were expressed in *Escherichia coli* with compromised solubility. Consequently, studies on the structure-guided enhancement of existing D-HYDs by molecular engineering and immobilization as well as identification of novel D-HYDs with specific substrate profile and stability have also been conducted [21–25].

Conventional screening is still a promising way to identify biocatalysts from natural sources [26]. To obtain a new D-HYD with different substrate specificity in the hydrolysis of 5′-

monosubstituted hydantoins for the preparation of D-AAs, screening of laboratory-preserved potential HYD-producing strains were carried out in this study. Using primers designed according to the consensus sequence of D-HYDs, a D-HYD from *Pseudomonas fluorescens* (D-*Pf*HYD) was cloned and heterogeneously expressed in *E. coli* for the first time. Various strategies were adopted to improve the soluble expression of D-*Pf*HYD. Additionally, the enzyme properties and potential application of D-*Pf*HYD were characterized. This work provides a new D-HYD for the biocatalytic synthesis of optically pure D-AAs.

Materials and Methods

Materials

Racemic and D-configured *p*-Hydroxyphenylglycine, valine, isoleucine, tryptophan, phenylalanine, and 2-chlorophenylglycine were of analytic grade and purchased from Sinopharm Chemical Regent Co., Ltd. PrimeSTAR HS and Taq polymerase, T4 DNA ligase, and five sets of recombinant plasmids harboring chaperone genes were obtained from TAKARA Co., Ltd. Primers were synthesized by Sangon Biotech Co., Ltd.

Synthesis of 5′-Monosubstituted Hydantoins and N-Carbamoyl-D-α-Amino Acids

Six *N*-carbamoyl-D-α-amino acids and 5′-monosubstituted hydantoins were synthesized using amino acid annulation method [27]. NaCNO and amino acids at a molar ratio of 1.5:1 were mixed and stirred at 80 °C for 2 h to get the *N*-carbamoyl-D-α-amino acids. Then, the reaction mixtures were acidified with HCl to pH of 2–3. Another two equivalent H_2SO_4 to *N*-carbamoyl-D-α-amino acids were added and stirred at 105 °C for 3 h. Reaction was slowly cooled at 4 °C for the crystallization of 5′-monosubstituted hydantoins. Then, the product was isolated and verified by HPLC and ^{1}H NMR (AVANCE III 400 MHz Digital NMR spectrometer, Germany). The molar yield and purity of 5′-monosubstituted hydantoins were shown in Table S1.

Screening of D-HYD-Producing Microorganisms

Twenty microorganisms preserved in our laboratory, including *Pseudomonas* sp., *Agrobacterium* sp., *Burkholderia* sp., *Bacillus* sp., *Rhodococcus* sp., *Enterobacter* sp., *Lactobacillus* sp., *Candida* sp., and *Delftia* sp., were cultured under their own optimal conditions and induced with 2 mM isobutylhydantoin when OD_{600} reached 1.0. After 48 h, the cells were harvested by centrifugation at 4 °C and 8000×*g* for 10 min and washed for three times with physiological saline. HYD activities were measured with 10 μmol isobutylhydantoin in 1.0 mL Tris–HCl buffer (pH 9.0, 100 mM) employing appropriate cells harvested from a 5-mL fermentation broth at 37 °C for 10 min. Reaction was stopped by addition of 100 μL trichloroacetic acid (10 % *v*/*v*) and centrifuged at 12000×*g* for 10 min. The upper phase was filtrated through a 0.22-μm filter and analyzed by reverse HPLC. Carbamoylase activity was determined with 10 μmol *N*-carbamoyl-D-α-isoleucine in 1.0 mL Tris–HCl buffer (pH 9.0, 100 mM) employing appropriate cells. After reaction, the mixture was centrifuged at 12000×*g* for 10 min; the supernatant was filtrated with a 0.22-μm filter and determined using *o*-phthalaldehyde (OPA) method.

General Activity Assay and HPLC Analysis

General D-HYD activity assay was performed in a 500-μL reaction mixture consisting of 10 μmol isobutylhydantoin dissolved in 490 μL Tris–HCl buffer (pH 9.0, 100 mM) and 10 μL enzyme solution and at 45 °C and 180 rpm for 10 min. Then, the reaction was stopped by addition of 100 μL trichloroacetic acid (10 % *v*/*v*) and centrifuged at 12000×*g* for 10 min. The upper phase was filtrated through a 0.22-μm filter and analyzed by reverse HPLC. One unit of D-HYD activity was defined as the amount of enzymes used for the production of 1 μmol *N*-carbamoyl-D-α-isoleucine. HPLC analysis of 5′-monosubstituted hydantoins, *N*-carbamoyl-D-α-amino acids, and D-amino acids were described as follows.

1. 5′-Monosubstituted hydantoins and *N*-carbamoyl-D-α-amino acids were quantified with reverse HPLC equipped with SunFire C-18 column (4.6 × 250 mm, 5 μm) with different ratios of methanol and ddH_2O at 1 mL min^{-1}, 30 °C, and 210 nm. The ratios and retention times are listed in Table S2.
2. D-amino acids (2 μL) were derived with 3 μL *o*-phthalaldehyde (0.1 g L^{-1} in methanol) and 5 μL sodium tetraborate (100 mM) and measured using HPLC equipped with Xbridge C18 column (4.6 × 250 mm, 5 μm) at 1 mL min^{-1}, 30 °C, and 338 nm. Buffer A (3 g L^{-1} sodium acetate, pH 7.2) and buffer B (methanol/acetonitrile/3 g L^{-1} sodium acetate = 2:2:1) were gradient-mixed with ratios of 85:15, 0:100, and 85:15 at time points of 0, 15, and 30 min, respectively.
3. Enantioselectivity of the produced D-amino acids were determined with HPLC equipped with OD-H column (4.6 × 250 mm, 5 μm) using isopropanol/hexane/trifluoroacetic acid (15:85:0.05) as eluent at 0.8 mL min^{-1}, 30 °C, and 210 nm.

Cloning and Expression of D-PfHYD-Coding Gene (hyd)

Genomic DNA of *P. fluorescens* CGMCC1.1802 was extracted and purified employing TIANamp Bacteria Kit and used as template. Primers I (forward GGTCATGCCTGCGA GGAACT, reverse TCAGCGTTTTCGGCAGTGG) was adopted to get the full open reading frame. Then, primers II (forward CTAGCTAGCATGTCGCTG TTGATCCGTG, reverse CCCAAGCTTTCAGCGTTTTACGGCAGT) was used to get the target D-*Pf*HYD-coding gene (*hyd*). The PCR product and expressing vector pET28a were double-digested with *Nhe*I and *Hin*dIII and ligated with T4 DNA ligase at 16 °C for 6 h, transformed into *E. coli* BL21(DE3). The resultant pET28-*hyd* was extracted and further transferred into *E. coli* BL21(DE3) harboring different chaperones, pGRO7 (GroES-GroEL), pGRO7-KJE8 (GroES-GroEL & DnaK-DnaJ-GrpE), pKJE7 (DnaK-DnaJ-GrpE), pGRO7-TF2 (GroES-GroEL & Tigger), and pTF16 (Tigger) (Table S3). The recombinant *E. coli* BL21(DE3) with pET28-*hyd*, pET28-*hyd*/pGRO7, pET28-*hyd*/pGRO7-KJE8, pET28-*hyd*/pKJE7, pET28-*hyd*/pGRO7-TF2, and pET28-*hyd*/pTF16 was cultured at 37 °C in LB medium supplemented with kanamycin and chloramphenicol. When the OD_{600} reached 0.6, 0.1 mM IPTG and different inducers were added to induce the expression of *hyd* and chaperones (Table S3). Afterwards, the cultures were cultured at 25 °C for 6 h. Cells were harvested by centrifugation (8000×*g*, 10 min, 4 °C) and washed for two times. Cells were resuspended in Tris–HCl buffer (pH 9.0, 100 mM) and disrupted by ultrasonication (work 1 s, interval 3 s for 15 min) or homogenized by nano homogenize machine (AH-BASICI, ATS Engineering Inc., Canada). The supernatant

was harvested by centrifugation (12000×*g*, 10 min, 4 °C) to get the crude enzyme solutions of D-*Pf*HYD. The whole cells were lyophilized to powder under vacuum and stored at 4 °C for further use.

Purification of D-PfHYD

Cells harboring D-*Pf*HYD were resuspended in binding solution and disrupted as mentioned above. Crude enzyme solution was obtained by centrifugation to remove the cell debris. After being loaded on the HisTrap FF column, D-*Pf*HYD was washed by elution buffer at about 400 mM imidazole. To remove the residual imidazole, the collected eluents were concentrated and went through a HiTrap Desalting column. Purified D-*Pf*HYD was verified by SDS-PAGE and stored at −80 °C with 20 % (*v*/*v*) glycerol for further use. Molecular weight of D-*Pf*HYD was determined using Superdex 200 10/300 GL column.

Effect of pH, Temperature, and Metal Ions on the Activity of D-PfHYD

The pH profile of purified D-*Pf*HYD was determined using the standard activity assay protocol in the following buffers: sodium phosphate buffer (pH 6.0–8.0, 100 mM), Tris–HCl (pH 8.0–9.5, 100 mM), and glycine-NaOH (pH 9.0–10.0, 100 mM). The optimum temperature of D-*Pf*HYD was also measured under the above-mentioned standard condition at various temperatures (4–70 °C). Thermostability of D-*Pf*HYD was investigated by incubating purified D-*Pf*HYD solution (0.1 mg mL^{-1}) at 45, 50, 55, and 60 °C. About 30 μL D-*Pf*HYD was withdrawn from the mixture, and the residual activity was determined using the standard assay method. All the activities were assayed in triplicate.

The effects of various metal ions and additives (including Mn^{2+}, Zn^{2+}, Ca^{2+}, Ba^{2+}, Co^{2+}, Ni^{2+}, Al^{3+}, Pb^{2+}, Fe^{2+}, Fe^{3+}, and EDTA) on D-*Pf*HYD activity were examined by adding each compounds in the enzyme solution (1 mg mL^{-1}) for 60 min at 30 °C, and the enzyme activities were measured under the standard condition. Control was performed in the absence of any test compound. All the activities were assayed in triplicate.

Substrate Specificity and Kinetic Analysis

Substrate specificity of D-*Pf*HYD toward six 5′-monosubstituted hydantoins was characterized, including isopropylhydantoin, isobutylhydantoin, p-hydroxyphenylhydantoin, phenylmethylhydantoin, 2-chlorobenzenehydantoin, and indomethylhydantoin. Kinetic constants of D-*Pf*HYD toward the above hydantoins were determined at different concentrations (0.1, 0.5, 1.0, 2.0, 5.0, 7.5, 10.0, and 20.0 mM). K_m and V_{max} were calculated according to Lineweaver-Burk plot.

Chemoenzymatic Synthesis of D-Isoleucine

Semi-preparative synthesis of D-isoleucine was carried out in a 100-mL whole-cell biocatalytic system. Ten micromolars of isobutylhydantoin was added in the 100-mL Tris–HCl buffer (pH 9.0, 100 mM). Reaction was started by addition of 0.10 g dry cell weight, shaken at 45 °C. To promote the racemization of isobutylhydantoin, reaction was maintained at pH 9.0. Samples were removed, and conversion was analyzed by HPLC. Because the solubility of *N*-carbamoyl-D-isoleucine was over 200 mM under pH > 12 while low under pH 2–4, *N*-

carbamoyl-D-isoleucine was recovered by simply adjusting the pH of reaction mixture. After termination, the cell debris was separated by adjusting pH to higher than 12 and centrifugation at 12000×*g* for 10 min, and the *N*-carbamoyl-D-isoleucine was harvested by adjusting the pH to lower than 3.0 and centrifugation at 12000×*g* for 10 min. Then, *N*-carbamoyl-D-isoleucine was dissolved in 2 M HCl and further hydrolyzed by slowly adding 0.1 M $NaNO_2$ to 1.2 equivalent of *N*-carbamoyl-D-isoleucine [28]. D-Ile was crystallized and isolated in the ice bath with agitation. The pH of the mixture was adjusted to 7.0 using 2 M NaOH and flowed through cationic chromatography (001 × 7001 × 7FC001 × 7 MB). D-Ile was washed with ethanol and evaporated under vacuum at 60 °C. Then, the liquid was stored at 4 °C for the recrystallization of D-Ile. Enantiomeric excess (*ee*) value was calculated according to the following formula:

$$\text{Enantiomeric excess } (\boldsymbol{ee}) = \frac{\boldsymbol{A}_{D\text{–}Ile} - \boldsymbol{A}_{L\text{–}Ile}}{\boldsymbol{A}_{D\text{–}Ile} + \boldsymbol{A}_{L\text{–}Ile}} \times 100\% \quad (1)$$

$\boldsymbol{A}_{\text{D-Ile}}$ and $\boldsymbol{A}_{\text{L-Ile}}$ refer to the peak area of D-Ile and L-Ile, respectively.

Results and Discussion

Screening of D-Hydantoinase-Producing Microorganisms

Twenty microorganisms preserved in our laboratory were screened for D-hydantoinase activity toward 5′-monosubstituted hydantoins. It has been reported that hydantoins could be used as the sole carbon and/or nitrogen sources and that HYD is an inducible expression system [29]. Thus, a certain amount of isobutylhydantoin was supplemented at a logarithmic growth phase to induce the expression of HYD. *P. fluorescens* CGMCC 1.1802, *Burkholderia cepacia* CGMCC 1.1813, *Pseudomonas putida* 901, *P. putida* KT2440, *Agrobacterium* sp. F1, and *Pseudomonas aeruginosa* 1–3 displayed obvious hydrolysis activity toward 5′-monosubstituted hydantoins, whereas none of the tested strains showed detectable carbamoylase activity. The HYD activity and enantioselectivity of these strains are listed in Table 1. All the strains exhibited D-configured selectivity. Among them, *P. putida* KT2440 displays the highest activity toward isobutylhydantoin (53.9 U L^{-1}), while *P. fluorescence* CGMCC 1.1802 shows the highest activity toward *p*-hydroxyphenylhydantoin (20.4 U L^{-1}). The *ee* value of *P. fluorescence* CGMCC 1.1802 toward isobutylhydantoin and *p*-hydroxyphenylhydantoin are 98.6 and 98.5 %, respectively, ranking the highest enantioselectivity. In 1986, the D-HYD-producing *P. fluorescens* was first reported by Morin and coworkers, and the specific activities toward isopropylhydantoin and *p*-hydroxyphenylhydantoin were 0.126 and 0.133 U mg^{-1} wet cells [29]. However, its exact enantioselectivity has not been reported, and the active D-HYD from *P. fluorescens* has not been heterogeneously expressed. Consequently, the identification, expression, and characterization of the D-HYD from *P. fluorescens* are of special interest.

Cloning of D-PfHYD-Coding Gene from *Pseudomonas fluorescens*

The D-hydantoinase-coding gene, *hyd*, was amplified from the genome of *P. fluorescens* according to the deduced hydantoinase sequence. The *hyd* gene is 1440 bp in length and was deposited in GenBank under the accession no. KF268426.1. The resultant PCR product

Table 1 Screening of microorganisms for hydantoinase activity toward isobutylhydantoin and *p*-hydroxyphenylhydantoin

Microorganism	Isobutylhydantoin			*p*-Hydroxyphenylhydantoin		
	Activity [U L^{-1}]	*ee* [%]	Config. [D/L]	Activity [U L^{-1}]	*ee* [%]	Config. [D/L]
Pseudomonas fluorescens CGMCC1.1802	23.4 ± 0.5	98.6	D	20.4 ± 0.3	98.5	D
Burkholderia cepacia CGMCC1.1813	3.17 ± 0.30	97.6	D	3.69 ± 0.31	97.3	D
Pseudomonas putida 901	4.25 ± 0.87	96.9	D	1.12 ± 0.51	96.7	D
Pseudomonas putida KT2440	53.9 ± 0.9	97.9	D	8.43 ± 0.94	98.2	D
Agrobacterium sp. F1	23.5 ± 0.39	95.7	D	8.00 ± 0.73	95.9	D
Pseudomonas aeruginosa 1–3	11.3 ± 0.17	95.8	D	3.19 ± 0.17	95.8	D

was ligated into pET28a and transferred into *E. coli* BL21(DE3). After being induced with IPTG, D-HYD was mostly expressed in insoluble form (Fig. S2). The activity of the recombinant D-*Pf*HYD toward isobutylhydantoin was 5.34 U mg^{-1} crude extract. This recombinant D-HYD from *P. fluorescens* was designated as D-*Pf*HYD.

Phylogenetic analysis was conducted to understand the evolution relationship of D-*Pf*HYD and other known HYDs. The highest sequence identity (83 %) was found with dihydropyrimidinase from *P. putida* (Uniprot No. Q59699). In addition, D-*Pf*HYD shows 55, 46, 32, and 28 % sequence identities to dihydropyrimidinases from *Sinorhizobium meliloti* (Uniprot No. Q0PQZ5), *Brevibacillus agri* (A846U5), *Bacillus halodurans* (Q5DLU2), and *Arthrobacter aurescens* (P81006), which are efficient hydantoianses in the hydrolysis of 5′-monosubstituted hydantoins. Several hydrolases have been reported with hydantoin hydrolysis activity, including amidohydrolase, dihydropyrimidase/hydantoinase, allantoinase, and dihydroorotase, which belong to the cyclic amidase superfamily containing 22 potential subfamilies. Most of the reported hydantoin hydrolysis reactions are catalyzed by dihydropyrimidinases, which are involved in the physiological metabolism of pyrimidine. According to the phylogenetic tree (Fig. 1), D-*Pf*HYD displays a close relationship to dihydropyrimidase/hydantoinase, whereas it is distinct from allantoinase (ALN, AllB, LhyD, and FeAllB) and dihydroorotase (PyrC, Ura4). Based on the above analysis, we conclude that D-*Pf*HYD should be classified into dihydropyrimidinase family.

Sequence consensus was also analyzed between D-*Pf*HYD and similar proteins. As illustrated in Fig. 2, the tested D-HYDs display high primary sequence and secondary structure similarities. The structure and the detailed mechanism of D-HYD from *Sinorhizobium meliloti* (SmelDhp) have been uncovered [30]. SmelDhp is a sandwich structure with a catalytic TIM barrel domain which is an eightfold repetition of α/β motif wrapped in a circular fashion [30]. According to the structure of SmelDhp, all the catalytic residues are conserved in D-*Pf*HYD, including His59, His61, Lys150, His183, His239, and Asp 316, which participate in the hydrolysis reaction by interaction with metal ions and hydantoin substrates through the carbamate group, amide nitrogen and carbonyl oxygen.

Characterization of Purified D-PfHYD

Recombinant D-*Pf*HYD with His-tag at *N*-terminus was purified to homogeneity via nickel column affinity chromatography. A single band migrated on SDS-PAGE around 55 kDa indicates the successful purification of D-*Pf*HYD (Fig. S1). The molecular weight of D-

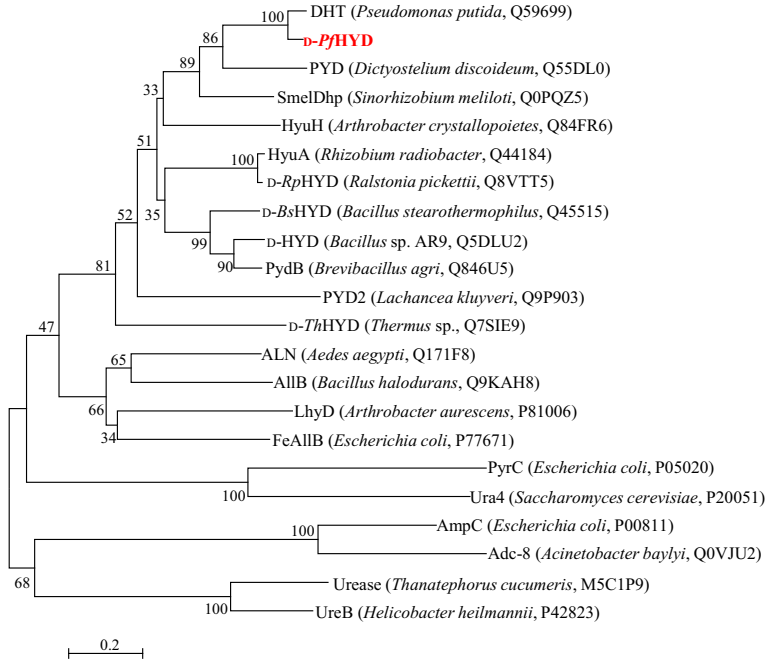

Fig. 1 Phylogenetic analysis of D-*Pf*HYD and closely related proteins. The phylogenetic tree was constructed with MEGA 6.0 software by a neighbor-joining method. The bootstrap values were based on 10,000 replicates

*Pf*HYD subunit calculated based on SDS-PAGE is in agreement with its theoretical mass of 54.4 kDa. After desalting, the purified D-*Pf*HYD was subjected to Superdex chromatography, resulting in a molecular weight of 215 kDa. Therefore, the newly identified D-*Pf*HYD is a homotetramer, in consistence with most of the reported D-hydantoinase. The specific activity of the purified D-*Pf*HYD is 20.9 U mg^{-1}, with purification fold of 3.91 and 66.6 % activity recovery (Table S4).

The D-*Pf*HYD prefers basic buffer and displays the highest activity at pH 9.0 (Fig. 3a) and could retain more than 90 % of activity over a pH range from 8.5 to 9.5. At pH lower than 7.5, the activity decreased sharply to around 5 % at pH 6.0. Basic preference of D-*Pf*HYD is advantageous for the "hydantoinase process," since the 5′-monosubstituted hydantoins could be spontaneously racemized, which is important to achieve an ideal 100 % conversion. The introduction of a hydantoin racemase would complicate the biocatalytic process considering the enzyme preparation cost and the matching kinetic properties between racemase and HYD. It has been reported that D-*p*-hydroxylphenylhydantoin could be spontaneously racemized into DL-*p*-hydroxyphenylhydantoin with racemization constants (k_{rac}) of 2.26 h^{-1} and corresponding half-life time ($t_{1/2,rac}$) of 0.12 h at pH 8.0 [31]. However, the racemization of aliphatic 5′-monosubstituted hydantoins, such as isobutylhydantoin, is much more difficult than aromatic 5′-monosubstituted hydantoins. The k_{rac} and $t_{1/2,rac}$ values of isobutylhydantoin are 0.043 h^{-1} and 15.84 h, respectively, under the same condition [31].

Effect of temperature on the activity of purified D-*Pf*HYD was carried out at 4–70 °C (Fig. 3b).The optimal temperature of D-*Pf*HYD is around 60 °C. At 30 and 45 °C, relative activity of 29.4 and 62.0 % were remained. The purified D-*Pf*HYD enzyme solution (0.1 mg mL^{-1}) was incubated at 45, 50, 55, and 60 °C. The residual activities of D-*Pf*HYD

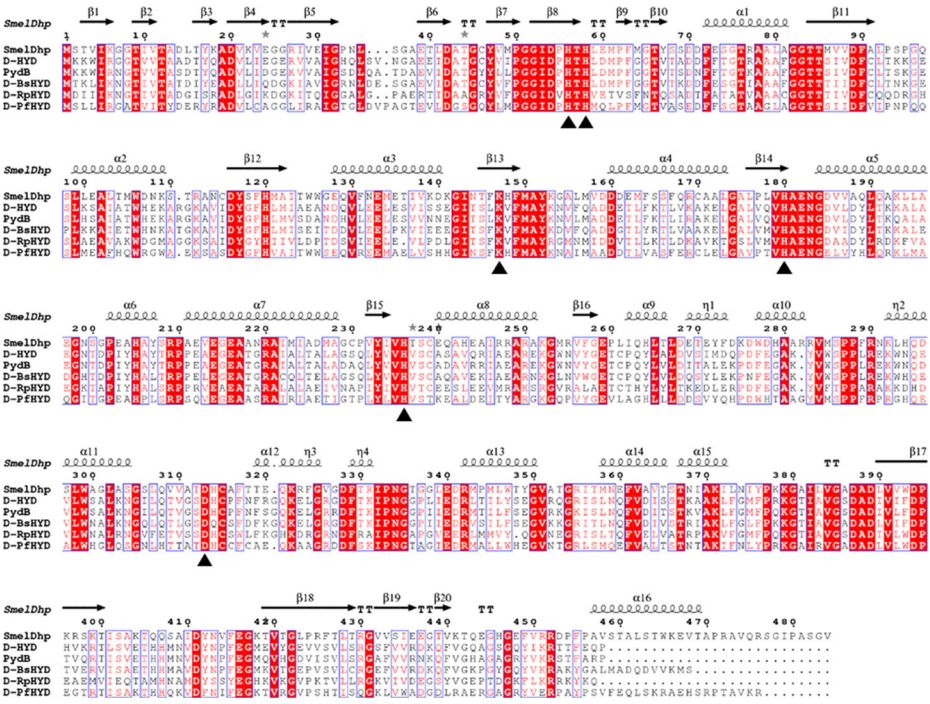

Fig. 2 Multiple sequence alignment of D-*Pf*HYD and similar hydantoinases. SmelDhp (*Sinorhizobium meliloti*, Uniprot accession no. Q0PQZ5); D-HYD (*Bacillus* sp., Q5DLU2); PydB (*Brevibacillus Agri*, Q846U5); D-BsHYD (*Bacillus stearothermophilus*, Q45515); and D-RpHYD (*Ralstonia pickettii*, Q8VTT5). (▲) conserved catalytic residues

under different temperatures were monitored every 30 min. According to the inactivation curves (Fig. 3c), the residual activities decreased quickly at the initial 2 h and remained stable to 8 h. The half-lives of D-*Pf*HYD at 45, 50, 55, and 60 °C were calculated to be 5.61, 2.23, 1.44, and 0.78 h, respectively. Considering that D-*Pf*HYD could retain a high activity at 45 °C and the spontaneous racemization rate of 5′-monosubstitttuted hydantoins requires high temperature, 45 °C was chosen as the suitable temperature for the enzymatic hydrolysis of hydantoins.

Most of the D-HYDs were reported to be dependent on divalent cations (Zn^{2+}, Ni^{2+}, Co^{2+}, or Mn^{2+}, etc.). Metal ions could interact with residues such as His58, His60, His183, His239, and His319 according to the structure of *Bacillus stearothermophilus* D-HYD (D-*Bs*HYD) [12]. The metal ion dependence of D-*Pf*HYD was explored by incubation of various common divalent cations or EDTA at 30 °C for 60 min. Control was carried out under the same condition without any additives and regarded as 100 %. As shown in Fig. 3d, zinc ion severely inhibited the activity of D-*Pf*HYD (10 % residual activity), which is different from other D-HYDS. Under the existence of Mn^{2+}, Fe^{2+}, and Fe^{3+}, D-*Pf*HYD displayed about 20 % higher activity than did the control. No metal ions were found to significantly activate the enzyme. Addition of metal chelating agents, EDTA, has little inhibitory effect on the activity of D-*Pf*HYD. Mukohara and coworkers have proven that Ni^{2+}, Co^{2+}, and Mn^{2+} could significantly stimulat the activity of D-*Bs*HYD by 1.6, 2.2, and 1.9 times [12]. However, EDTA could partially inhibit the activity of D-*Bs*HYD, which is similar to D-*Pf*HYD. It is speculated that certain uncommon divalent cations might relate to the metal dependence of D-*Pf*HYD.

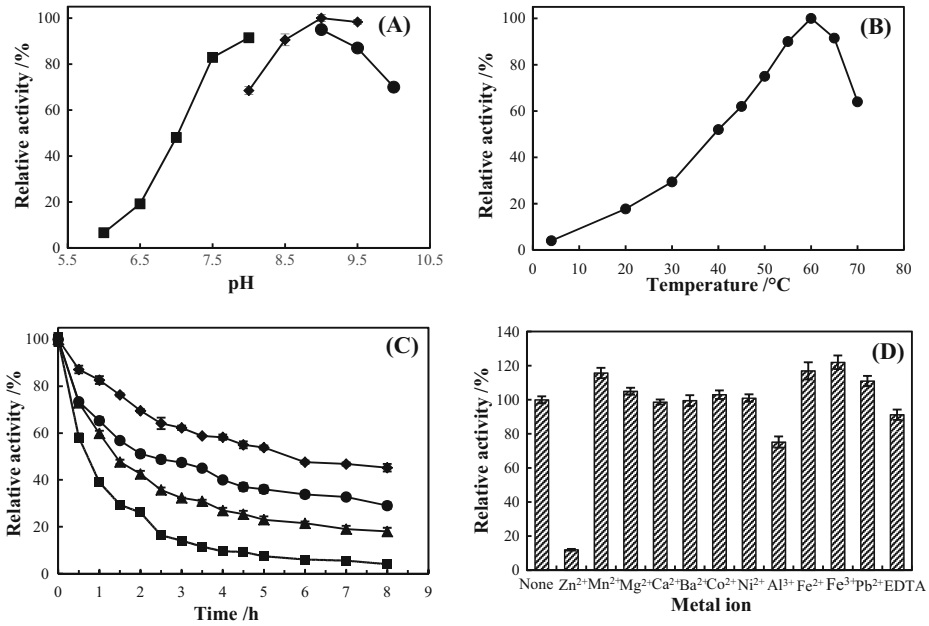

Fig. 3 Characteristics of purified D-*Pf*HYD. **a** pH profile: *filled squares* PBS, *filled diamonds* Tris–HCl, and *filled circles* glycine-NaOH. **b** Temperature profile. **c** Thermostability: *filled diamonds* 45 °C, *filled circles* 50 °C, *filled triangles* 55 °C, and *filled squares* 60 °C. **d** Metal ion dependence

Substrate Specificity

Different hydantoins with various 5′-monosubstituents, such as isopropylhydantoin, isobutylhydantoin, *p*-hydroxyphneylhydantoin, phenylmethylhydantoin, 2-chlorobenzenehydantoin, and indolmethylhydantoin, were used to characterize substrate specificity of D-*Pf*HYD. The kinetic constants of D-*Pf*HYD toward the six hydantoins were listed in Table 2. The lowest K_m (4.42 mM) and the highest k_{cat} (391 s^{-1}) were detected for isobutylhydantoin, which could be hydrolyzed into D-isoleucine. For *p*-hydroxyphenylhydantoin, which is a substrate for an important pharmaceutical precursor D-4-hydroxyphenylglycine, the K_m and k_{cat} are 7.52 mM and 74.2 s^{-1}, respectively. The k_{cat}/K_M values toward isopropylhydantoin and isobutylhydantoin are 10.1 and 88.5 s^{-1} mM^{-1}, higher than those of phenylmethylhydantoin (0.31 s^{-1} mM^{-1}), 2-chlorobenzenehydantoin (0.04 s^{-1} mM^{-1}), and indolmethylhydantoin (0.31 s^{-1} mM^{-1}). The results indicate that D-*Pf*HYD prefers aliphatic to the aromatic 5′-monnosubstitutented hydantoins. Most of D-HYDs originating from *Pseudomonas* sp. display higher catalytic activity toward aromatic 5′-monosubstituted hydantoins. It has been reported that crude extract of *P. fluorescens* exhibited similar activity to isopropylhydantoin (0.126 U mg^{-1}) and *p*-hydroxyphenylhydantoin (0.133 U mg^{-1}) [29], which is consistent with the similar k_{cat} values toward isopropylhydantoin (77.3 s^{-1}) and *p*-hydroxyphenylhydantoin (74.2 s^{-1}) in this study. Substrate specificity analysis provides guidance for the potential application of D-*Pf*HYD in the synthesis of chiral D-AAs.

Table 2 Steady-state kinetic constants of purified D-*Pf*HYD toward 5′-monosubstituted hydantoins

Substrate	Structural formula	K_m [mM]	k_{cat} [s^{-1}]	k_{cat}/K_m [$s^{-1}\cdot mM^{-1}$]
Isopropylhydantoin	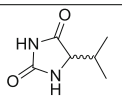	7.63 ± 0.21	77.3 ± 3.3	10.1
Isobutylhydantoin	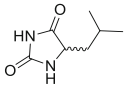	4.42 ± 0.41	391 ± 6	88.5
p-Hydroxyphenylhydantoin	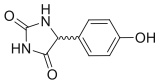	7.52 ± 0.23	74.2 ± 2.1	9.87
Phenylmethylhydantoin	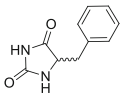	9.49 ± 0.07	2.91 ± 0.04	0.31
2-Chlorobenzenehydantoin	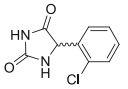	8.57 ± 0.19	0.37 ± 0.05	0.04
Indolmethylhydantoin	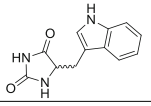	4.64 ± 0.37	1.43 ± 0.10	0.31

Enhancing the Soluble Expression of D-PfHYD

To achieve an efficient and the economic synthesis of chiral D-AAs, the preparation cost of the biocatalyst should be low. However, many D-HYDs were reported to be expressed as insoluble protein in *E. coli* [7]. Various strategies have been developed to increase the soluble expression level or operational stability, including various host strains, vectors, in vivo immobilization, or surface display [23–25]. Majority of D-*Pf*HYDs were also expressed in insoluble form (Fig. S2). We thus adopted different methods to improve the soluble expression of D-*Pf*HYD.

Firstly, the original ribosom binding site (RBS) of D-*Pf*HYD (GAGGAA) was introduced to replace the RBS of *E. coli* (AAGGAG) since different RBS might play different roles in the protein expression. However, the total expression level of D-*Pf*HYD was decreased and almost no HYD activity was detected which might be ascribed to the incompatibility of heterogeneous RBS in *E. coli* BL21(DE3). Replacing a T7 promoter with T5 could often result in slower expression rate and enhanced soluble expression. Here, pQE-80L harboring a T5 promoter was attempted. After IPTG induction, most of D-*Pf*HYD remained as insoluble protein. The specific activity was 5.58 U mg^{-1}, similar to that of pET28 harboring a T7 promoter (5.34 U mg^{-1}). Chaperones have been reported to be effective in assisting protein folding into their functional structure during protein synthesis [32]. To promote the correct folding of D-*Pf*HYD, five sets of molecular chaperones were coexpressed with D-*Pf*HYD in *E. coli*, including pGRO7 (GroES-GroEL), pKJE7 (DnaK-DnaJ-GrpE), pTF16 (Tigger), pGRO7-KJE8 (GroES-GroEL & DnaK-DnaJ-GrpE), and pGRO7-TF2 (GroES-GroEl & Tigger) (Fig. 4). After induction, the soluble expression of recombinant D-*Pf*HYD was analyzed by SDS-PAGE and activity assay. Under the assistance of GroES-GroEL, D-*Pf*HYD was expressed mostly in soluble form, and the highest specific activity of 12.0 U mg^{-1} was reached, representing 2.3 times of the control (5.34 U mg^{-1}). The specific activities of D-

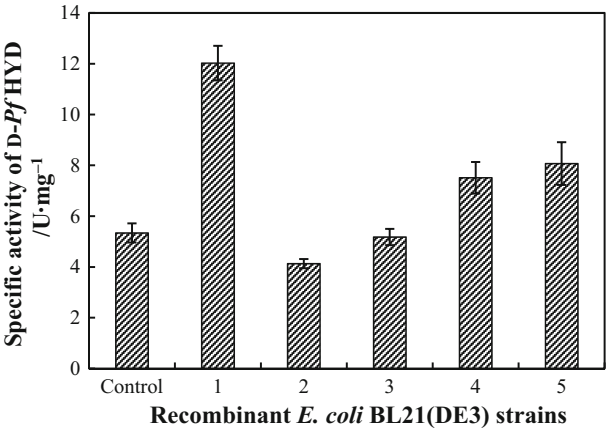

Fig. 4 Effect of different chaperones on the activity of D-*Pf*HYD expressed in *E. coli* BL21(DE3). *Control* without chaperone, *1* pGRO7 (GroES-GroEL), *2* pKJE7 (DnaK-DnaJ-GrpE), *3* pTF16 (Tigger), *4* pGRO7-KJE8 (GroES-GroEL & DnaK-DnaJ-GrpE), and *5* pGRO7-TF2 (GroES-GroEl & Tigger)

*Pf*HYD coexpressed with DnaK-DnaJ-GrpE and Tigger were 4.13 and 5.18 U mg^{-1}, respectively. After combining DnaK-DnaJ-GrpE and Tigger with GroES-GroEL, the soluble expression of D-*Pf*HYD was increased (Fig. S2), and the specific activities were enhanced to 7.51 and 8.07 U mg^{-1}, respectively. It is known that GroES-GroEL could recognize and correct the hydrophobic region of the miss-folded protein by encapsulation and/or iterative annealing models. Consequently, *E. coli* BL21(DE3) harboring pET28-*hyd*/pGRO7 (GroES-GroEL) was selected for the production of recombinant D-*Pf*HYD.

Chemoenzymatic Synthesis of D-Isoleucine

The potential application of recombinant D-*Pf*HYD in the synthesis of D-isoleucine was investigated (Fig. 5). In a 100-mL reaction system, 100 mM isobutylhydantoin was hydrolyzed into *N*-carbamoyl-D-isoleucine with 98.2 % conversion by employing only 0.1 g dry cells of recombinant *E. coli* BL21(DE3)-pET28-*hyd*/pGRO7 within 27 h. The hydrolysis reaction rate of D-

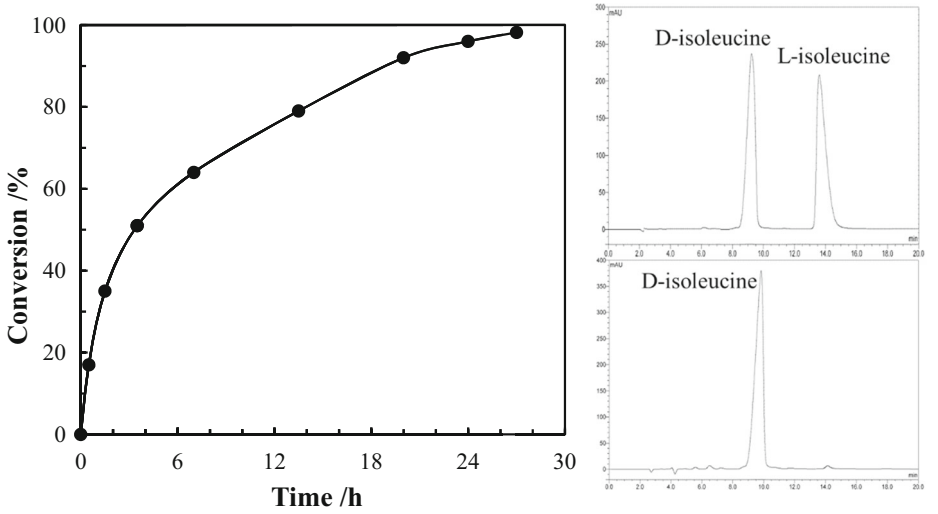

Fig. 5 Chemoenzymatic synthesis of D-isoleucine using recombinant *E. coli* BL21(DE3)/pET28-*hyd*/pGRO7

*Pf*HYD was affected by the slow racemization rate of isobutylhydantoin, which led to a relatively slow conversion rate. After combining with a chemical method for the hydrolysis of the carbamoyl group [28], all the *N*-carbamoyl-D-isoleucine was further converted into D-isoleucine with *ee* and isolation yield of 98.7 and 78.3 %, respectively. The substrate to biocatalyst ratio was calculated to be 15.6. The recombinant D-*Pf*HYD was proven to be efficient in the preparation of D-isoleucine. Further study on the cascade reaction system catalyzed by D-*Pf*HYD along with hydantoin racemase and carbamoylase is currently undergoing.

Conclusion

A D-hydantoinase-producing *P. fluorescens* CGMCC1.1802 was identified. The active D-hydantoinase was overexpressed in *E. coli* BL21(DE3) and designated as D-*Pf*HYD. Sequence analysis reveals that D-*Pf*HYD belongs to the dihydropyrimidase family. D-*Pf*HYD displayed the highest activity at pH 9.0 and 60 °C. Mn^{2+}, Fe^{2+}, and Fe^{3+} could activate the activity of D-*Pf*HYD. Purified D-*Pf*HYD showed substrate preference toward aliphatic 5′-monosubstituted hydantoins. Soluble expression of D-*Pf*HYD was achieved by co-expression with chaperone GroES-GroEL. Employing 1.0 g L^{-1} recombinant *E. coli* dry cells, 100 mM isobutylhydantoin was converted into D-isoleucine with *ee* and isolation yield of 98.7 and 78.3 %, respectively, and a substrate to biocatalyst ratio of 15.6. This study proves the potential application of D-HYD from *P. fluorescens* in the synthesis of unnatural D-amino acids.

Acknowledgments We are grateful to the National Natural Science Foundation of China (21276112, 21506073), the Natural Science Foundation of Jiangsu Province (BK20150003), the Fundamental Research Funds for the Central Universities (JUSRP51409B), the Program of Introducing Talents of Discipline to Universities (111-2-06), and a project funded by the Priority Academic Program Development of Jiangsu Higher Education Institutions for the financial support of this research.

Compliance with Ethical Standards

Conflicts of Interest All the authors certify that this manuscript is original and has not been published and will not be submitted elsewhere for publication while being considered by Applied Biochemistry and Biotechnology. And the study is not split up into several parts to increase the quantity of submissions and submitted to various journals or to one journal over time. No data have been fabricated or manipulated (including images) to support your conclusions. No data, text, or theories by others are presented as if they were our own. The submission has been received explicitly from all co-authors. And authors whose names appear on the submission have contributed sufficiently to the scientific work and therefore share collective responsibility and accountability for the results. The authors declare that they have no conflict of interest. This article does not contain any studies with human participants or animals performed by any of the authors. Informed consent was obtained from all individual participants included in the study.

References

1. Gao, X. Z., Ma, Q. Y., & Zhu, H. L. (2015). Distribution, industrial applications, and enzymatic synthesis of D-amino acids. *Applied Microbiology and Biotechnology, 99*, 3341–3349.
2. Zhang, J., Xu, Y. & Li, R. (2013). Preparation method of aspoxicillin. *China Patent.* 103333180A.
3. Walters, D. E. (1995). Using models to understand and design sweeteners. *Journal of Chemical Education, 72*, 680–683.

4. Omura, T. & Furukawara, T. (2014). Oil-in-water type emulsion skin cosmetic. *United States Patent*. 8607750B2.
5. Altenbuchner, J., Siemann-Herzberg, M., & Syldatck, C. (2001). Hydantoinases and related enzymes as biocatalysts for the synthesis of unnatural chiral amino acids. *Current Opinion in Biotechnology, 12*, 559–563.
6. Bommarius, A. S., Schwarm, M., & Drauz, K. (1998). Biocatalysis to amino acid-based chiral pharmaceuticals—examples and perspectives. *Journal of Molecular Catalysis B: Enzymatic, 5*, 1–11.
7. Burton, S. G., & Dorrington, R. A. (2004). Hydantoin-hydrolysing enzymes for the enatioselective production of amino acids: new insights and applications. *Tetrahedron: Asymmetry, 15*, 2737–2741.
8. Jiang, M., Shang, L. A., Wei, P., Yu, R. H., Shen, N., Ouyang, P. K., & Chang, H. N. (2007). Pilot-scale production of D-p-hydroxyphenylglycine from DL-5-p-hydroxyphenylhydantoin by Burkholderia cepacia JS-02. *Enzyme and Microbial Technology, 41*, 407–412.
9. Syldatk, C., May, O., Altenbuchner, J., & Mattes, R. (1999). Microbial hydantoinases-industrial enzymes from the origin of life? *Applied Microbiology and Biotechnology, 51*, 293–309.
10. Zhang, X. Y., Niu, L. X., Shi, Y. W., & Yuan, J. M. (2008). The flexibility of the non-conservative region at the C terminus of D-hydantoinase from *Pseudomonas putida* YZ-26 is extremely limited. *Applied Biochemistry and Biotechnology, 144*, 237–247.
11. Durham, D. R., & Weber, J. E. (1995). Properties of D-hydantoinase from *Agrobacterium tumefaciens* and its use for the preparation of *N*-carbamyl D-amino acids. *Biochemical and Biophysical Research Communications, 216*, 1095–1100.
12. Mukohara, Y., Ishikawa, T., Watabe, K., & Nakamura, H. (1994). A thermostable hydantinase of *Bacillus stearothermophilus* NS1122A: cloning, sequencing, and high expression of the enzyme gene, and some properties of the expressed enzyme. *Bioscience, Biotechnology, and Biochemistry, 58*, 1621–1626.
13. Xu, Z., Liu, Y. Q., Yang, Y. L., Jiang, W. H., Arnold, E., & Ding, J. P. (2003). Crystal structure of D-hydantoinase from *Burkholderia pickettii* at a resolution of 2.7 Å: insights into the molecular basis of enzyme thermostability. *Journal of Bacteriology, 185*, 4038–4049.
14. May, O., Siemann, M., Pietzsch, M., Kiess, M., Mattes, R. & Syldatk, C. (1997) Substrate-dependent enantioselectivity of a novel hydantoinase from *Arthrobacter aurescens* DSM 3745: Purification and characterization as new member of cyclic amidases. *61*, 1–13.
15. Latacz, G., & Kiec-Kononowicz, K. (2014). Biotransformation of new racemic (R, S)-5-benzylhydantoin derivatives by D-hydantoinases from Adzuki bean. *Biocatalysis and Biotransformation, 32*, 117–124.
16. Su, T. M., & Yang, Y. S. (2000). Identification, purification, and characterization of a thermophilic imidase from pig liver. *Protein Expression and Purification, 19*, 289–297.
17. Ogawa, J., & Shimizu, S. (2002). Industrial microbial enzymes: their discovery by screening and use in large-scale production of useful chemicals in Japan. *Current Opinion in Biotechnology, 13*, 367–375.
18. Siemann, M., Alvarado-Marín, Á., Pietzsch, M., & Syldatk, C. (1999). A D-specific hydantoin amidohydrolase: properties of the metalloenzyme purified from *Arthrobacter crystallopoietes. Journal of Molecular Catalysis B: Enzymatic, 6*, 387–397.
19. Shi, Y. W., Niu, L. X., Feng, X., & Yuan, J. M. (2006). Purification, enzymatic properties of a recombinant D-hydantoinase and its dissociation by zinc ion. *World Journal of Microbiology and Biotechnology, 22*, 675–680.
20. Runser, S., & Ohleyer, E. (1990). Properties of the hydantoinase from *Agrobacterium* sp. IP I-671. *Biotechnology Letters, 12*, 259–264.
21. Cheon, Y. H., Park, H. S., Lee, S. C., Lee, D. E., & Kim, H. S. (2003). Structure-based mutational analysis of the active site residues of D-hydantoinase. *Journal of Molecular Catalysis B: Enzymatic, 26*, 217–222.
22. Lin, C. C., Liu, T. T., Kan, S. C., Zang, C. Z., Yeh, C. W., Wu, J. Y., Chen, J. H., Shieh, C. J., & Liu, Y. C. (2013). Production of D-hydantoinase via surface display and self-cleavage system. *Journal of Bioscience and Bioengineering, 116*, 562–566.
23. Chen, S. Y., Chien, Y. W., & Chao, Y. P. (2014). In vivo immobilization of D-hydatoinase in *Escherichia coli. Journal of Bioscience and Bioengineering, 118*, 78–81.
24. Kim, G. J., Lee, D. E., & Kim, H. S. (2001). High-level expression and one-step purification of cyclic amidohydrolase family enzymes. *Protein Expression and Purification, 23*, 128–133.
25. Chern, J. T., & Chao, Y. P. (2005). Chitin-binding domain based immobilization of D-hydantoinase. *Journal of Biotechnology, 117*, 267–275.
26. Ogawa, J., & Shimizu, S. (1999). Microbial enzymes: new industrial application from traditional screening methods. *Trends in Biotechnology, 17*, 13–20.
27. Ohishi, T., Nanba, H., Sugawara, M., Izumida, M., Honda, T., Mori, K., Yanagisawa, S., Ueda, M., Nagashima, N., & Inoue, K. (2007). Enantioselective synthesis of D- and L-α-methylcysteine with hydantoinase. *Tetrahedron Letters, 48*, 3437–3440.
28. Nandanwar, H. S., Prajapati, R., & Hoondal, G. S. (2013). (D)-*p*-Hydroxyphenylglycine production by thermostable D-hydantoinase from *Brevibacillus parabrevis*-PHG1. *Biocatalysis and Biotransformation, 31*, 22–32.

29. Morin, A., Hummel, W., & Kula, M. R. (1986). Production of hydantoinase from *Pseudomonas fluorescens* strain DSM84. *Applied Microbiology and Biotechnology, 25*, 91–96.
30. Martínez-Rodríguez, S., Martínez-Gómez, A. I., Clemente-Jiménez, J. M., Rodríguez-Vico, F., García-Ruíz, J. M., Javier, F., Heras-Vázquez, L., & Gavira, J. A. (2010). Structure of dihydropyrimidinase from *Sinorhizobium meliloti* CECT4114: new features in an amidohydrolase family member. *Journal of Structural Biology, 169*, 200–208.
31. Clemente-Jiménez, J. M., Martínez-Rodríguez, S., Rodríguez-Vico, F., & Heras-Vázquez, F. J. L. (2008). Optically pure α-amino acids production by the "hydantoinase process". *Recent Patents on Biotechnology, 2*, 35–46.
32. Dobson, C. M. (2003). Protein folding and misfolding. *Nature, 426*, 884–890.